Korean J. Chem. Eng., **27**(3), 848-853 (2010)
DOI: 10.1007/s11814-010-0140-8

Performance characteristics of NO removal by cobalt diethylenetriamine solution

Houzhang Tan*,†, Jinchao Wei, Yunbai Luo**, and Ping Yu****

*School of Energy and Power Engineering, Xi'an Jiaotong University, Xi'an 710049, China
**College of Chemistry and Molecule Science, Wuhan University, Wuhan 430072, China
(*Received 9 December 2008 • accepted 9 October 2009*)

Abstract−The cobalt(II) diethylenetriamine ($[Co(dien)_2]^{2+}$) complex is a newly developed metal thiochelate for the removal of NO from flue gas. The performance characteristics of NO absorption into $[Co(dien)_2]^{2+}$ solution were studied in a stirred reactor. The experimental results showed that this absorption could be regarded as fast pseudo-mth-order reaction and the reaction rate could be expressed as second-order with respect to NO concentration and first-order with respect to $[Co(dien)_2]^{2+}$ concentration. The enhancement factor was 1609.1 at the $[Co(dien)_2]^{2+}$ concentration of 0.01 mol/L. Its optimal absorption conditions were temperature 50 °C, NO concentration 540 ppm, $[Co(dien)_2]^{2+}$ concentration 0.02 mol/L and O_2 concentration 6%, which were determined by orthogonal experiment.

Key words: Nitric Oxide, Absorption, Cobalt Chelate, Diethylenetriamine

INTRODUCTION

It is generally accepted that nitric oxides (NO_x), in addition to sulfur dioxide (SO_2), are the main cause of environmental pollution such as acid rain, acid smog, and a reduction in the ozone layer. So the removal of nitrogen oxides is strongly required. A good denitrification process is selective catalytic reduction (SCR). It can catalytically reduce NO_x to N_2 and H_2O by reacting it with NH_3 [1,2]. This process has a leading position on the current denoxing market. The drawbacks are its relatively high costs and poisoning of the catalyst by arsenic or alkali compounds in the fly ash [3,4].

Many alternatives to the SCR process that are based on wet scrubbing have been widely studied in the US [5-8], Japan [9,10] and Netherlands [11-13]. Flue gas contains several hundred ppm of NO_x and most of the NO_x is in the form of nitric oxide (NO). The solubility of NO is very low in aqueous solution, but can be considerably improved by adding metal chelate complexes to solution to bind NO forming nitrosyl metal complexes. These complexes, such as ferrous and cobalt chelates, can coordinate NO and be regenerated by different methods. Long et al. pointed out that NO could be removed from exhausted gas streams by $[Co(en)_3]^{2+}$ (en=Ethylenediamine) or $[Co(NH_3)_6]^{2+}$ solution which could realize the oxidation and absorption of nitric oxide in the same reactor [14-16]. This process was superior to the method using Fe(II)-EDTA (EDTA=ethylenediaminetetraacetate) solution because these cobalt chelates are substantially more resistant to oxidation than Fe(II)-EDTA [17]. However, ethylenediamine and ammonia as ligands have low flash point and high volatility, which causes difficulty in transportation and waste raw materials. Moreover, it is difficult to prepare $[Co(en)_3]^{2+}$ and $[Co(NH_3)_6]^{2+}$ solutions because the direct blend of the two raw materials will bring a great deal of precipitation. Considering that diethylenetriamine has a high flash point (94 °C) and is easily and widely used as a ligand, the authors investigated the ability of $[Co(dien)_2]^{2+}$ solution to remove NO from flue gas. NO can react with $[Co(dien)_2]^{2+}$ to form a nitrosyl complex as Eq. (1).

$$NO+[Co(dien)_2]^{2+} \rightarrow [Co(dien)_2NO]^{2+} \quad (1)$$

In the present work, the mass transfer rates of NO into the aqueous $[Co(dien)_2]^{2+}$ solution were studied in a stirred tank. In addition, orthogonal design was employed to evaluate the relative importance of various operating parameters and optimize absorption conditions.

EXPERIMENTAL SECTION

1. Materials

Cobalt (II) chloride hexahydrate ($CoCl_2 \cdot 6H_2O$, AR) and diethylenetriamine ($C_4H_{13}N_3$, CP) were purchased from Sinopharm Chemical Reagent Co., Ltd, China. NO (1,000 vppm in N_2), N_2 (>99.99%)

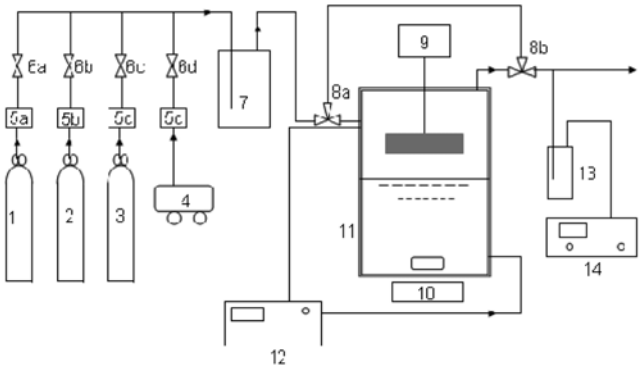

Fig. 1. Schematic representation of the experimental apparatus.

1. NO gas cylinder	8a, 8b. Three way valves
2. N_2 gas cylinder	9. Driving motor
3. CO_2 gas cylinder	10. Magnetic plate
4. Air compressor	11. Stirred cell reactor
5a, 5b, 5c, 5d. Gas flowmeters	12. Water bath
6a, 6b, 6c, 6d. Open/close valves	13. Dryer
7. Mixer	14. NO analyzer

†To whom correspondence should be addressed.
E-mail: tanhz@mail.xjtu.edu.cn

Table 1. Dimensions and characteristics of the stirred cell reactor

Total reactor volume (m^3)	4.24×10^{-4}
Interfacial area (m^2)	28.2×10^{-4}
Gas impeller (m)	Two-bladed turbine, $d=1\times10^{-2}$
n_G Gas stirrer (min^{-1})	0□300
n_L Liquid stirrer (min^{-1})	0□300

and CO_2 (>99%) were obtained from Oxygen Co., Ltd. of WISCO, China. Reverse osmosis water was applied to prepare the cobalt chelate solution.

2. Experimental Set-up

A schematic diagram of the experimental apparatus is shown in Fig. 1. The experiments were carried out in a glass stirred cell reactor. The cell has a water jacket through which water from a constant temperature bath is circulated to maintain the desired temperature. The inner diameter and height of stirred cell are 6 cm and 15 cm, respectively. A polytetrafluoroethylene turbine impeller was used to stir the gas phase, while a magnetic stirrer (2 cm) in combination with an external magnetic drive was used for the liquid phase. Typical dimensions of the stirred cell reactor are given in Table 1.

NO or CO_2 was diluted by N_2 to the desired concentrations in the mixing vessel before being fed to the stirred cell reactor. A continuous total gas flow rate was maintained at 400 ml/min. Gaseous NO was absorbed through the free gas-liquid interface. The concentration of NO was measured by Delta2000-CD-IV flue gas analyzer (York Instrument Ltd.). To protect the flue gas analyzer, the simulated gas was dried. The incoming NO concentration was measured just before the gas inlet, and the outlet concentration was measured just after the gas outlet. Three-way valves regulate the gas stream which should be analyzed.

The liquid phase was an aqueous solution of $[Co(dien)_2]^{2+}$. The $[Co(dien)_2]^{2+}$ solution was prepared by adding $CoCl_2{\cdot}6H_2O$ and dien with 1 : 2 stoichiometry. Unlike the gas phase, the solution was not flowed and used batchwise.

RESULTS AND DISCUSSION

1. Liquid-Side and Gas-Side Mass Transfer Coefficients

The liquid-side mass transfer coefficient (k_L) of the cell was determined by measuring the rate of physical absorption of pure CO_2 into water at 50 °C and then correlated to the liquid phase stirring speed, n_L. The k_L value was independent of the liquid flow rate under the experimental conditions.

$$k_{L,CO_2-H_2O}=3.204\times10^{-7}n_L^{0.7098}(m/s) \quad (2)$$

The gas-side mass transfer coefficient, k_G, was determined by absorption of dilute CO_2 into an aqueous 1.5 mol/L NaOH solution at 50 °C. Under such conditions, the overall mass transfer coefficient, K_G, is approximately equal to the gas-side mass transfer coefficient, $K_G=k_G$, the gas-side mass transfer coefficient was correlated to the gas-phase stirrer speed n_G by

$$k_{G,CO_2}=3.072\times10^{-8}n_G^{0.5275}(mol/(m^2\cdot s\cdot Pa)) \quad (3)$$

The values of liquid- and gas-side mass transfer coefficients for NO can be estimated by Eqs. (4) and (5), respectively [18].

$$k_{L,NO}=k_{L,CO_2}(D_{NO-H_2O}/D_{CO_2-H_2O})^{2/3} \quad (4)$$

$$k_{G,NO}=k_{G,CO_2}(D_{NO-N_2}/D_{CO_2-N_2})^{2/3} \quad (5)$$

Where D_{NO-H_2O} and $D_{CO_2-H_2O}$ can be calculated from the Wilke-Chang equation [19] and their values are 4.47×10^{-9} and 3.59×10^{-9} $m^2{\cdot}s^{-1}$, respectively, at 50 °C. D_{NO-N_2} and $D_{CO_2-N_2}$ can be calculated from the Chapman-Enskog equation[16] and their values are 2.34×10^{-5} and 1.76×10^{-5} $m^2{\cdot}s^{-1}$, respectively, at 50 °C.

In our case, the value of $k_{L,NO}$ is 1.348×10^{-5} m/s at 160 rpm and 50 °C and $k_{G,NO}$ is 7.526×10^{-7} mol/($m^2{\cdot}s{\cdot}$Pa) at 300 rpm and 50 °C.

2. Determination of the Kinetic Regime

The reaction rate between the absorbed component NO and the reactant cobalt diethylenetriamine can be described with an expression of the form:

$$r=k_{mn}C_{NO}^{m}C_{[Co(dien)_2]^{2+}}^{n} \quad (6)$$

To identify the kinetic regime, a series of systematic experiments was conducted according to the principle proposed by Levenspiel and Godfrey [20] as shown in Table 2.

2-1. Effect of Liquid Volume

The experiments were performed at 50 °C. The inlet NO concentration was 400 ppm. The gas-liquid interfacial area was 28.2×10^{-4} m^2. $[Co(dien)_2]^{2+}$ concentration was 0.015 mol/L. As shown in Fig. 2, the reaction rates varied from 3.082×10^{-6} mol/($s{\cdot}m^2$) to 3.128×

Table 2. Factors influencing absorption reaction

Parameters instruction	Symbols	Zone of mass transfer and reaction kinetics							
		A	B	C	D	E	F	G	H
Concentration of reactant B in bulk of liquid	C_{BL}	+	–	+	+	?	?	+	+
Intensity of pressure of A in bulk of gas	P	+	+	+	+	?	?	+	+
Interfacial areas	A	+	+	+	+	+	+	+	–
Liquid volume	V_L	–	–	–	–	+	+	+	+
Liquid-side mass transfer coefficient	k_L	+	–	+	–	?	?	+	–
Gas-side mass transfer coefficient	k_G	+	+	+	+	?	?	+	+
Second order rate constant	k_2	–	–	+	+	?	?	+	+

A-instantaneous reaction; B-instantaneous reaction in diffusion film; C-fast reaction; D-fast pseudo-m^{th}-order reaction; E-moderately fast reaction; F-moderately fast pserdo-*mth*-oder reaction; G-slow reaction in bulk liquid; H-very slow reaction in bulk liquid; "+" effected factor; "–" not effected by factor; "?" may be effect factor, but rate equation will not be changed

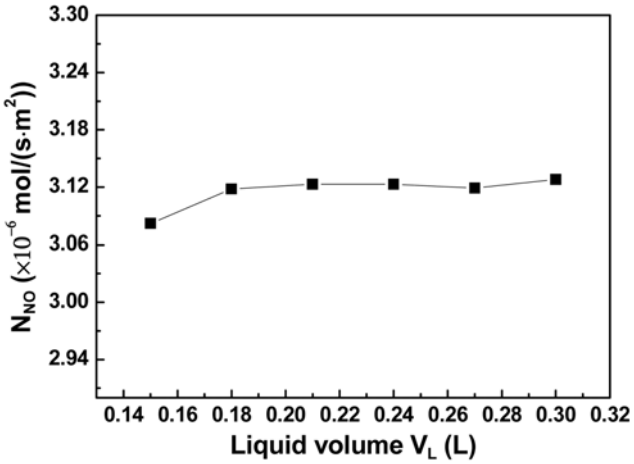

Fig. 2. Effect of liquid volume on absorption rate.

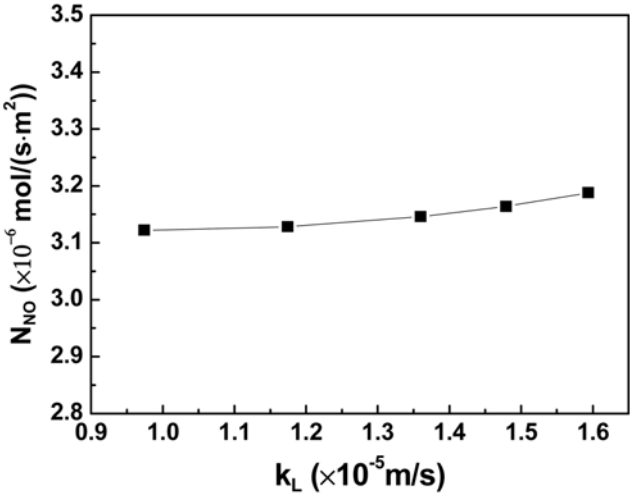

Fig. 3. Effect of liquid-side mass-transfer coefficient on absorption rate.

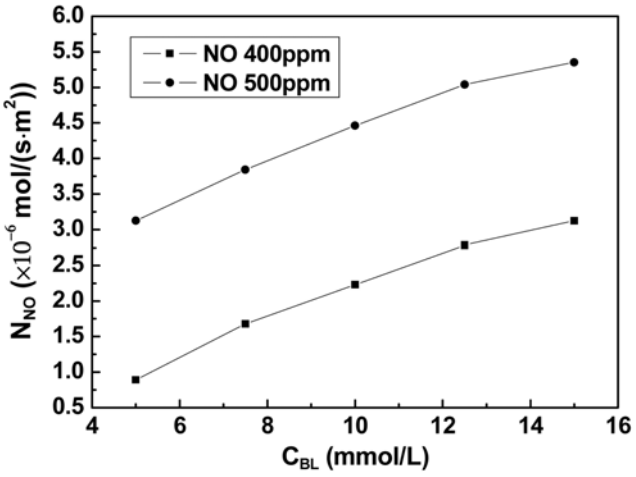

Fig. 4. Effect of $[Co(dien)_2]^{2+}$ concentration on absorption rate.

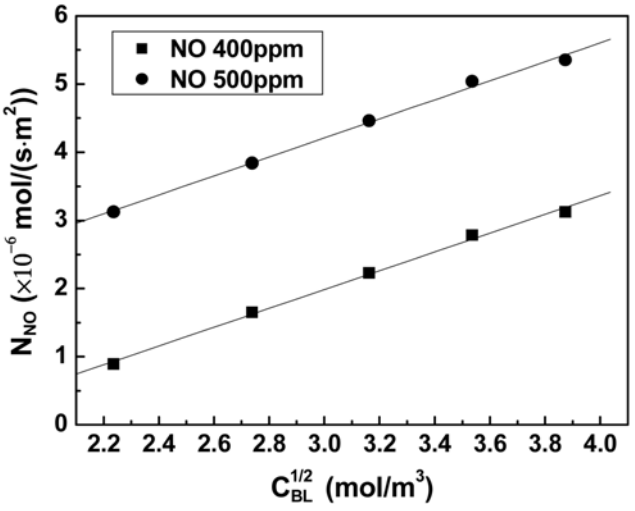

Fig. 5. Relationship between N_{NO} and $C_{BL}^{1/2}$ under different NO concentration.

10^{-6} mol/(s·m^2) as liquid volumes in the stirred cell increased from 0.15 to 0.3 L, which indicated that the nitric oxide absorption rate was almost independent of the liquid volume. Consequently, the kinetic regimes of E, F, G and H can be eliminated.

2-2. Effect of Liquid-side Mass Transfer Coefficient

The influence of liquid-side mass-transfer coefficient k_L, which is a function of apparatus hydrodynamics, was evaluated by varying the impeller speed in the stirred reactor as indicated in Fig. 3. The inlet NO concentration was 405 ppm. The gas-liquid interfacial area was 28.2×10^{-4} m^2. The liquid in the stirred cell was 240 mL, 0.015 mol/L $[Co(dien)_2]^{2+}$ solution. The absorption rate varied from 3.122×10^{-6} mol/(s·m^2) to 3.188×10^{-6} mol/(s·m^2) as the liquid-side mass-transfer coefficient increased from 0.974×10^{-5} m/s to 1.954×10^{-5} m/s. It can be clearly seen that the absorption rate of NO is independent of k_L under these conditions. Therefore, the kinetic regimes of A and C can be eliminated.

2-3. Effect of $[Co(dien)_2]^{2+}$ Concentration

Fig. 4 shows the effect of $[Co(dien)_2]^{2+}$ concentration on NO absorption rate. The experimental conditions for the measurements were 50 °C, 240 mL $[Co(dien)_2]^{2+}$ solution and inlet NO concentration 400 and 500 ppm, respectively. It can be seen from Fig. 4 that the NO absorption rate is increased by increasing the $[Co(dien)_2]^{2+}$ concentration. Since the absorption rate of NO is proportional to C_{BL}, the kinetic regime of B can be eliminated.

After the above discussion, a conclusion can be drawn that the NO absorption into $[Co(dien)_2]^{2+}$ solution can be regarded as fast pseudo-mth-order reaction when $[Co(dien)_2]^{2+}$ concentration is below 15 mmol/L.

3. Determination of Reaction Order and Rate Constant

For a fast pseudo mth-order of reaction, the absorption rate equation of NO can be written as [21]:

$$N_{NO}=\sqrt{\frac{2}{m+1}k_{m1}D_{NO}C_i^{m+1}C_{BL}} \tag{7}$$

On the basis of the mass transfer model (Eq. (7)), there should be a linear relationship between NO absorption rate and square root of the concentration of $[Co(dien)_2]^{2+}$. This prediction was confirmed by the results shown in Fig. 5.

Eq. (7) can be rearranged to become:

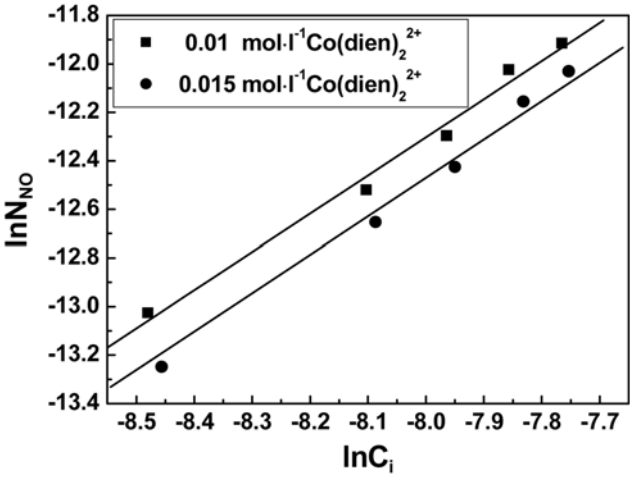

Fig. 6. Relationship between $\ln N_{NO}$ and $\ln C_i$ under different [Co (dien)$_2$]$^{2+}$ concentration.

$$\ln N_{NO} = \frac{1}{2}\ln\frac{2k_{m1}D_{NO}C_{BL}}{m+1} + \frac{m+1}{2}\ln C_i \quad (8)$$

Where

$$C_i = H_{NO}(p_G - N_{NO}/k_{G,NO}) \quad (9)$$

The value of (m+1)/2 can be obtained from the slope of a plot of $\ln N_{NO}$ vs $\ln C_i$. The experiments were run at 50 °C, 0.01 and 0.015 mol// [Co(dien)$_2$]$^{2+}$ solution 240 mL and different inlet NO concentration. The resulting plot is shown in Fig. 6, where the slope is found to be 1.5, so the reaction order can be determined to be m=2. The average rate constant k_{m1}, which can be calculated from the intercepts, is 5.912×10^7(m^3/mol)^2/s. Then the rate equation (Eq. (10)) was obtained by substituting the value of m, average rate constant and liquid phase diffusivity into Eq. (7).

$$N_{NO} = \sqrt{0.176C_i^3 C_{BL}} \quad (10)$$

4. Determination of Enhancement Factor

The enhancement factor can be evaluated from Eq. (11). The values were calculated from the measured values of absorption rate

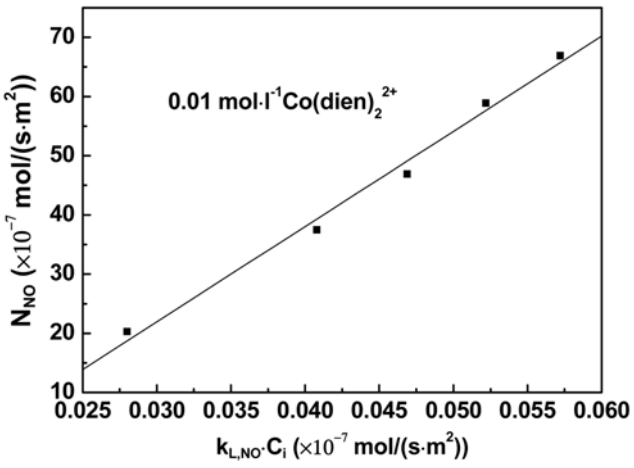

Fig. 7. Relationship between N_{NO} and $K_{L,NO}C_i$.

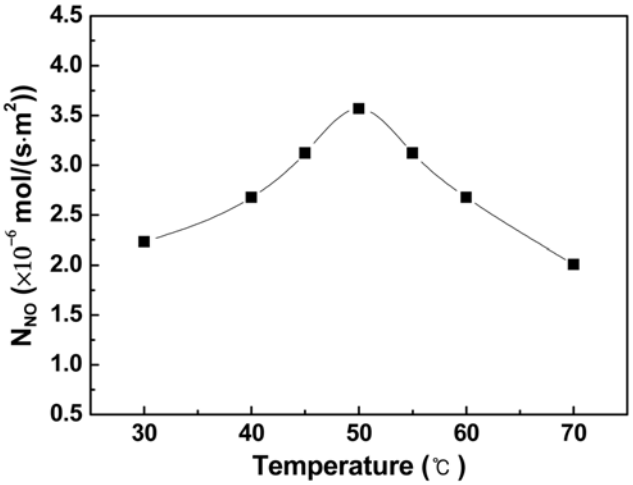

Fig. 8. Effect of temperature on NO absorption rate.

N_{NO}, liquid phase mass transfer coefficient without chemical reaction, $k_{L,NO}$, and estimated NO concentration of gas-liquid interface.

$$E = N_{NO}/(k_{L,NO}C_i) \quad (11)$$

The relationship between N_{NO} and $k_{L,NO}\cdot C_i$ is shown in Fig. 7. These experiments were performed at 50 °C for both gas and liquid phase, with different inlet NO concentrations and 0.01 mol/L [Co (dien)$_2$]$^{2+}$ solution. It can be seen from Fig. 7 that the slope of line is 1609.1, implying that the enhancement factor is 1609.1.

5. Effect of Temperature on NO Absorption Rate

A group of experiments was performed to investigate the effect of temperature (30-70 °C) on the absorption rate of NO. It can be seen from Fig. 8 that NO absorption rate increases with temperature when the temperature is below 50 °C. However, it decreases as the temperature increases further above 50 °C.

Dynamically, the reaction rates between NO and [Co(dien)$_2$]$^{2+}$ increase with temperature; thus, the absorption of NO increases with temperature. On the other hand, a negative influence of raising the temperature on NO absorption performance should be mentioned. Namely, the physical solubility of NO in aqueous solution decreases

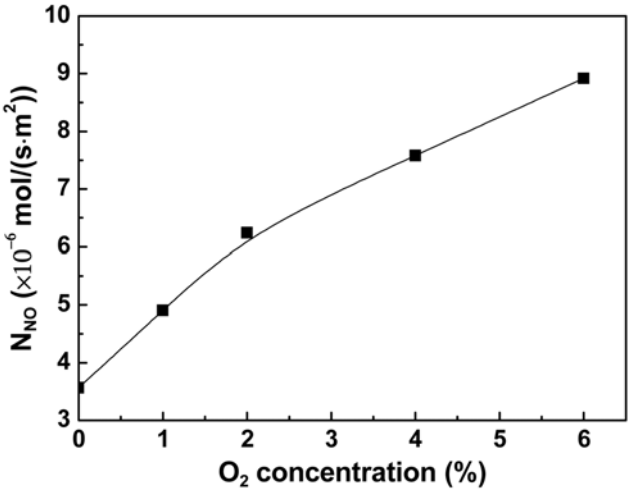

Fig. 9. Effect of inlet oxygen concentration on absorption rate.

as the temperature is increased. When the temperature is below 50 °C, the NO removal is governed mainly by the reaction step, so NO removal efficiency increases with rising temperature. After the temperature is above 50 °C, the physical solubility of NO controls mainly the NO removal. Therefore, the higher the temperature, the lower the NO removal rate. So, there is an optimal temperature for the absorption of NO by $[Co(dien)_2]^{2+}$ solution.

6. Effect of Inlet Oxygen Concentration on Absorption Rate

The effect of varying inlet O_2 concentrations on NO absorption rate is shown in Fig. 9. Under aerobic condition, the dissolved oxygen (Eq. (12)), in equilibrium with oxygen in the feed gas, activated by $[Co(dien)_2]^{2+}$ solution (Eqs. (13) and (14)), oxidizes nitric oxide to soluble nitrite (NO_2^-) and nitrate (NO_3^-) quickly (Eq. (15)). So NO absorption rate increases with O_2 concentration.

$$O_2(g) \leftrightarrow O_2(aq) \quad (12)$$

$$[Co(dien)_2]^{2+} + O_2(aq) \rightarrow [Co(dien)_2]^{3+}(O_2^-) \quad (13)$$

$$[Co(dien)_2]^{2+} + [Co(dien)_2]^{3+}(O_2^-) \rightarrow (dien)_2Co^{3+}-O-O-Co^{3+}(dien)_2 \quad (14)$$

$$2(dien)_2Co^{3+}-O-O-Co^{3+}(dien)_2 + 2NO + H_2O \rightarrow 4[Co(dien)_2]^{3+} + NO_2^- + NO_3^- + 2OH^- \quad (15)$$

7. Orthogonal Experiment

To obtain the optimal absorption conditions for $[Co(dien)_2]^{2+}$ solution, orthogonal design was employed. Orthogonal design is a method of arranging experiments and analyzing data via orthogonal arrays. $L_9(3^4)$ orthogonal design was used in this experiment for optimization of absorption conditions including NO concentration, $[Co(dien)_2]^{2+}$ concentration, temperature and O_2 concentration. The results and statistical analysis of the orthogonal experiment are shown in Table 3. It can be seen that the △ for NO concentration and temperature have the highest and lowest value, respectively, which reveals that the influential extent of the affecting factors to the NO absorption is NO concentration>O_2 concentration>$[Co(dien)_2]^{2+}$ concentration> temperature. The results also indicate that the optimal absorption conditions were temperature 50 °C, NO concentration 540 ppm, $[Co(dien)_2]^{2+}$ concentration 0.02 mol/L and O_2 concentration 6%. Under the optimal absorption conditions, the absorption rate is 1.160×10^{-5} mol/(s·m^2), which is higher than the experiment No. 3 in Table 3.

CONCLUSIONS

The removal of NO by cobalt diethylenetriamine solution in this system can be regarded as fast pseudo-mth-order reaction. The reaction rate is expressed as second-order with respect to NO $[Co(dien)_2]^{2+}$ and first-order with respect to $[Co(dien)_2]^{2+}$ concentration. The absorption rate equation was found to be $N_{NO}=\sqrt{0.176C_i^3C_{BL}}$ at 50 °C under anaerobic condition. The enhancement factor is 1609.1 at the [Co $(dien)_2]^{2+}$ concentration of 0.01 mol/L.

The NO absorption rate increases with increasing NO, O_2 and $[Co(dien)_2]^{2+}$ concentration. The optimal temperature for NO absorption is 50 °C. To obtain the optimal absorption conditions, an orthogonal experiment was carried out and the results were temperature 50 °C, NO concentration 540 ppm, $[Co(dien)_2]^{2+}$ concentration 0.02 mol/L and O_2 concentration 6%. Under these optimal conditions, the absorption rate can reach up to 1.160×10^{-5} mol/(s·m^2).

ACKNOWLEDGMENT

The work is supported by the National Nature Science Foundation of China (NO. 50976086).

Table 3. The results and statistical analysis of the orthogonal experiment

No.	Factors				Results
	NO concentration (ppm)	$[Co(dien)_2]^{2+}$ concentration (mol/L)	Temperature (°C)	O_2 concentration (%)	NO absorption rate ($\times10^{-6}$ mol/(s·m^2))
1	275	0.005	60	4	3.568
2	405	0.005	40	2	4.014
3	540	0.005	50	6	8.474
4	275	0.01	50	2	3.568
5	405	0.01	60	6	6.69
6	540	0.01	40	4	7.805
7	275	0.02	40	6	4.906
8	405	0.02	50	4	7.359
9	540	0.02	60	2	7.582
K_1	12.042	16.056	16.725	19.178	
K_2	18.063	18.063	19.401	18.732	
K_3	23.861	19.847	17.840	20.070	
R_1	4.014	5.352	5.575	6.393	
R_2	6.021	6.021	6.467	6.244	
R_3	7.954	6.616	5.947	6.690	
△	3.940	1.264	0.892	0.446	
Ranking	1	2	3	4	

Ki represents the sum of NO absorption rate at level i ($\times10^{-6}$ mol/(s·m^2)); R_i represents the average NO absorption rate at level i ($\times10^{-6}$ mol/(s·m^2)); △=the max R_i minus the min R_i

NOMENCLATURE

C : concentration [mol·m^{-3}]
D : diffusion coefficient [m^2·s^{-1}]
E : enhancement factor
H : Henry's law constant [mol·m^{-3}·Pa^{-1}]
K_G : the overall mass transfer coefficient [mol·s^{-1}·m^{-2}·Pa^{-1}]
k_L : liquid-side mass transfer coefficient [m·s^{-1}]
k_G : gas-side mass transfer coefficient [mol·s^{-1}·m^{-2}·Pa^{-1}]
k_{mn} : rate constant of (m, n)th order reaction [(m^3·mol^{-1})$^{m+n-1}$·s^{-1}]
m : reaction order
N : absorption rate [mol·m^{-2}·s^{-1}]
n : reaction order
n_G : gas phase stirrer speed [rpm]
n_L : liquid phase stirrer speed [rpm]
p : partial pressure [Pa]
r : reaction rate [mol·m^{-3}·s^{-1}]

Subscripts

B : liquid-phase reactant B ($[Co(dien)_2]^{2+}$)
G : gas phase
i : gas-liquid interface
L : liquid phase

REFERENCES

1. M. Kang, J. H. Park and J. S. Choi, *Korean J. Chem. Eng*., **24**, 191 (2007).
2. J. Yao, J. S. Choi, K. S. Yang, D. Sun and J. S. Chung, *Korean J. Chem. Eng*., **23**, 888 (2006).
3. H. Zhang, H. Tong, S. Wang, Y. Zhuo, C. Chen and X. Xu, *Ind. Eng. Chem. Res*., **45**, 6099 (2006).
4. H. K. Lee, B. R. Deshwal and K. S. Yoo, *Korean J. Chem. Eng*., **22**, 208 (2005).
5. N. D. Hutson, R. Krzyzynska and R. K. Srivastava, *Ind. Eng. Chem. Res*., **47**, 5825 (2008).
6. K. J. Smith, S. Tseng and M. Babu, Proceedings of the 86th Air and Waste Management, Denver, USA (1993).
7. E. K. Pham and S. G. Chang, *Nature*, **369**, 139 (1994).
8. S. G. Chang and D. K. Liu, *Nature*, **343**, 151 (1990).
9. E. Sada, H. Kumazawa and H. Machida, *Ind. Eng. Chem. Res*., **26**, 2016 (1987).
10. M. Sakai, C. Su and E. Sasaoka, *Ind. Eng. Chem. Res*., **41**, 5029 (2002).
11. F. Gambardella, M. S. Alberts, J. G. M. Winkelman and E. J. Heeres, *Ind. Eng. Chem. Res*., **44**, 4234 (2005).
12. J. F. Demmink, I. C. F. van Gils and A. A. C. M. Beenackers, *Ind. Eng. Chem. Res*., **36**, 4914 (1997).
13. F. Gambardella, L. M. G. Sanchez, K. J. Ganzeveld, J. G. M. Winkelman and H. J. Heeres, *Chem. Eng. J*., **116**, 67 (2006).
14. X.-L. Long, W.-D. Xiao and W.-K.Yuan, *Ind. Eng. Chem. Res*., **44**, 4200 (2005).
15. X.-L. Long, W.-D. Xiao and W.-K.Yuan, *Ind. Eng. Chem. Res*., **43**, 4048 (2004).
16. X.-L. Long, W.-D. Xiao and W.-K.Yuan, *Ind. Eng. Chem. Res*., **44**, 686 (2005).
17. X.-L. Long, W.-D. Xiao and W.-K.Yuan, *Chemosphere*, **59**, 811 (2005).
18. E. Sada, H. Kumazawa, Y. Yamanaka, I. Kudo and T. Kondo, *J. Chem. Eng. Jpn*., **11**, 276 (1978).
19. R. B. Bird, W. E. Stewart and E. N. Lightfoot, Transport Phenomena, Wiley, NewYork (1960).
20. O. Levenspiel and J. H. Godfrey, *Chem. Eng. Sci*., **29**, 1723 (1974).
21. P. V. Danckwerts, Gas-Liquid Reaction, McGraw-Hill, New York, NY, 247 (1970).